

Effects of Planetary Migration on Natural Satellites of the Outer Planets

C. Beaugé¹

Observatorio Astronómico, Universidad Nacional de Córdoba, Laprida 854, (5000) Córdoba, Argentina
E-mail: beauge@oac.uncor.edu

F. Roig

Observatorio Nacional, Rua Gen. Jose Cristino 77, Rio de Janeiro, 20921-400 RJ, Brazil

and

D. Nesvorný

Department of Space Studies, Southwest Research Institute, 1050 Walnut Street, Suite 426, Boulder, Colorado 80302

Received December 4, 2001; revised March 15, 2002

Numerous studies in the past few years have analyzed possible effects of planetary migration on the small bodies of the Solar System (mainly asteroids and KBOs), with the double aim of explaining certain dynamical structures in these systems, as well as placing limits on the magnitude of the radial migration of the planets. Here we undertake a similar aim, only this time concentrating on the dynamical stability of planetary satellites in a migration scenario. However, different from previous works, the strongest perturbations on satellite systems are not due to the secular variation of the semimajor axes of the planets, but from the planetesimals themselves. These perturbations result from close approaches between the planetesimals and satellites.

We present results of several numerical simulations of the dynamical evolution of real and fictitious satellite systems around the outer planets, under the effects of multiple passages of a population of planetesimals representing the large-body component of a residual rocky disk. Assuming that this component dominated the total mass of the disk, our results show that the present systems of satellites of Uranus and Neptune do not seem to be compatible with a planetary migration larger than even one quarter that suggested by previous studies, unless these bodies were originated during the late stage of evaporation of the planetesimal disk. For larger variations of the semimajor axes of the planets, most of the satellites would either be ejected from the system or suffer mutual collisions due to excitation in their eccentricities. For the systems of Jupiter and Saturn, these perturbations are not so severe, and even large migrations do not introduce large instabilities.

Nevertheless, even a small number of 1000-km planetesimals in the region may introduce significant excitation in the eccentricities

and inclinations of satellites. Adequate values of this component may help explain the present dynamical distribution of distant satellites, including the highly peculiar orbit of Nereid.

© 2002 Elsevier Science (USA)

Key Words: celestial mechanics; jovian planets; satellites—General; planetesimals; Solar System—Origin.

1. INTRODUCTION

The formation of the outer planets can be separated into two distinct groups. On one hand, Jupiter and Saturn were formed in a gas-rich environment. This implied a relatively fast formation time on the order of 10^6 – 10^7 years (Pollack *et al.* 1996), a large proportion of volatile gaseous component in them (chemical composition similar to the Sun), and little or no remnant of the primordial accretion disk remained at 5–10 AU after the accretion process.

The formation of Uranus and Neptune apparently took different lines. According to Fernández and Ip (1984), the fact that the ratio of gaseous material to rocky material in these planets is only about 20% implies that these bodies formed primarily after the dissipation of the solar nebula and, thus, in a gas-free scenario. Practically all studies of planetary formation (from the pioneering work of Safronov onward) place the formation times of these bodies on the order of 10^8 – 10^9 years (if not longer). Formation in a gas-free scenario is different from that in a gas-rich scenario. In the gas-free scenario the efficiency of the accretion process is lower, and after the formation of the planets a significant portion of the original rocky disk may have survived in the region beyond 10 AU (see Thommes *et al.* 1999).

The interaction of the residual disk with the formed outer planets may have given origin to the so-called planetary migration.

¹ Present address: Instituto Nacional de Pesquisas Espaciais, Av. dos Astronautas 1758, (12227-010) São José dos Campos, SP, Brazil.

Due to the gravitational perturbations of the planets (primarily, close encounters) there was an exchange of energy and angular momentum between both populations. As a result, the disk of planetesimals was expelled from the system and the orbits of the planets suffered secular (and permanent) changes. According to Hahn and Malhotra (1999), if the total mass of the residual disk was equal to $50M_{\oplus}$, then the semimajor axis of Jupiter was decreased by a quantity on the order of 0.2 AU, while the orbits of Saturn, Uranus, and Neptune were pushed to outer values. In the case of Neptune, this change was large, on the order of 7 AU.

The main consequence of this planetary migration was a secular temporal change in the semimajor axes of the planets lasting $\approx 5\text{--}30$ Myr. To check this result, several studies were performed on the effects of such a variation on the orbits of small bodies of the Solar System, such as the asteroid belt, the Trojan group, and Kuiper belt objects. It seems that, depending on the magnitude, this migration is not only consistent with the dynamical structure of these systems but also may help to understand certain characteristics. Examples are the stirring of eccentricities in the Kuiper belt (Malhotra 1993, 1995) and asteroid belt (Gomes 1997), absence of bodies in the Thule group (Michtchenko, in preparation), and maybe even the difference between the L_4 and L_5 population in the Trojan swarm (Gomes 1998). It has also been proposed that the Lunar late heavy bombardment could have been triggered by the formation of Uranus and Neptune and the consequent migration of the jovian planets (Wetherill 1975, Levison *et al.* 2001).

It is important to stress, however, that all these works concentrate on the effects of the changes in semimajor axes of the planets according to an externally fixed function $a(t)$, and little has been discussed on the origin of this migration. We know that this orbital variation is due to close encounters of planetesimals with the planets. What is the effect of the same encounters on small bodies of the Solar System? This is the question we wish to address.

Among the “small bodies” whose stability may be affected by these close encounters, we will study the natural satellites of the outer planets. We wish to analyze the perturbative effects of the swing-bys of the planetesimals on the orbital motion of planetary satellites. However, before undertaking this study, the first question we must answer is the applicability of this physical system. During the planetary migration, were the satellites already formed? Was their dynamical structure (i.e., stability, resonance relations) the same as it is today? The main question is the formation time of the satellites versus the migration time of the planets. Let us discuss this briefly.

The satellites of the outer planets can be divided into two groups, each with distinct dynamical properties which probably reflect different formation mechanisms. The so-called *regular* satellites are located close to the primary and are characterized by orbits which are practically circular and planar with respect to the planet’s equator. It includes the large quasi-spherical bodies (such as the Galilean satellites) as well as the small bodies located at very small distances from the primary, such as

those found in the vicinity of the ring systems. The abundance of mean-motion resonances among them speaks of significant orbital variation due to tidal evolution; thus, their original semi-major axes could have been much different in the past. Notwithstanding this fact, it is very likely that their origin is primordial, and they were formed through direct accretion from the circumplanetary disk. It is interesting to note that even in the case of Uranus, whose obliquity is more than 90° , its inner satellites all lie very close to the equatorial plane. Thus, we may conclude that during the post-planetary formation migration process, at least as depicted by Fernández and Ip, Hahn and Malhotra, and others, these bodies were probably already present.

The second group of bodies is usually referred to as *irregular* satellites. They are located at large distances from the primary and their orbits are characterized by large eccentricities and/or inclinations. In most cases the orbits are retrograde. In principle, their dynamical properties are not very compatible with formation from the primordial disk, unless latter evolutionary mechanisms can account for their present orbits. To date, this seems unlikely. Although solar perturbations are important at these planetary distances, these effects are insufficient to cause such a large increase in peculiar velocities. For this reason, several authors have suggested that they were not originated from the circumplanetary disk but, rather, consist of exterior planetesimals captured by the planet (see Gladman *et al.* 2001 and references therein). Three different scenarios are possible. In the first, the capture occurred during the mass growth of the primary (e.g., Heppenheimer and Porco 1977), in which temporary gravitational trappings were made permanent by the increase in size of Hill radius. In the second, the capture also occurred in primordial times, only this time assisted by gas drag with the surrounding solar nebula (Pollack *et al.* 1979). Last of all, in the third scenario, capture was accomplished through collisions between two or more planetesimals experiencing hyperbolic fly-bys.

The first two alternatives are usually believed to be applicable only to Jupiter and Saturn, since Uranus and Neptune are missing gas envelopes. Even in the case of both larger planets, the first hypothesis is usually thought of as unlikely since gravitational capture during formation times generally yields retrograde and not direct orbits, especially if the planetary mass increased very fast (on the order of 10^4 years). However, this is not necessarily the rule. Recent simulations by Nesvorný *et al.* (2002) seem to indicate that slow gas contraction in a cold disk can in fact give origin to distant prograde bodies.

Finally, the collisional hypothesis for satellite capture is also plausible, although perhaps not probable. The possible existence of dynamical “families” among them (Gladman *et al.* 2001) seems to support a collisional scenario. However, it must be noted that the members of many of these families have very low relative velocities (on the order of 10–40 m/s), and thus consistent with the idea that at least the parent body was already bounded to the planet prior to the fragmentation. Observational evidence also questions a collisional origin. As an example, recent spectroscopic studies of Nereid (Brown *et al.* 1998) seem

to indicate that this satellite was formed in a circumplanetary environment rather than being a captured object.

In fact, Nereid has always been a puzzle. Even though it has a prograde orbit, it is located at very large distances from the primary and has the largest eccentricity ($e \approx 0.75$) among irregular satellites. To add to the confusion, Triton, located much closer to the planet, moves in a retrograde orbit. Goldreich *et al.* (1989) have suggested that the dynamical characteristics of Nereid could be explained considering perturbative effects of Triton in past times. In this scenario, Nereid is a primordial body but Triton was originally a planetesimal captured from a heliocentric orbit. Dissipation due to tides raised on Neptune caused Triton's orbit to evolve toward its present state. During this evolution, Triton perturbed Nereid, thus accounting for this satellite's highly eccentric and inclined orbit.

In conclusion, although a primordial origin for the regular satellites is fairly agreed upon, the same does not apply to the irregular group. However, even in this case the balance seems presently shifted toward gravitational capture during the formation of the planet itself. If this were the case, it is interesting to note that, although these bodies cannot be thought of as primordial in a strict sense, their capture must have occurred before the end of the formation of the planets. Chronologically then, they may even predate the inner regular satellites themselves.

From this discussion it seems likely that at least the inner group of bodies (and perhaps the irregular group) already existed at the time planetary formation ended. How does the formation of the satellites relate with the timescale of the migration of the outer planets? First, it is important to differentiate between radial motion of planetary embryos and what is commonly referred to as planetary migration. The former (which we may call "embryonic migration") is common in all accretion processes of planetary formation and occurs throughout the whole formation time of the planet. As mentioned by Ida *et al.* (2000) and Bryden *et al.* (2000), this secular variation of the semimajor axes of the embryos is driven by accretion/scattering in an asymmetrical planetesimal distribution and is thus independent of the other giant planets.

The second type of orbital drift, what is usually referred to as "planetary migration" (e.g., Fernández and Ip and Hahn and Malhotra), is of a different nature. It is believed to have occurred after the formation of the planets and caused by the interactions of *several* planets with the residual planetesimal disk. This disk no longer contributed significantly to the accretion process and thus the interaction was pure scattering. Of course it is very probable that both models of migration were part of a single process that we simply separate chronologically; Hahn and Malhotra's model is simply that part which occurred after the end of the formation of the planets.

From all these considerations we can summarize that the aim of our study will be to analyze the effects of the post-formation planetary migration on satellite orbits, trying to deduce what is its maximum allowed magnitude consistent with the observed distribution of bodies around the outer planets. This manuscript

is divided as follows: In Section 2 we discuss the method of numerical integration employed in this work. Section 3 discusses the results of our simulation of planetary migration. We also analyze the close encounters themselves, with special emphasis on the distribution of planetocentric orbits as a function of the pericentric distance. Section 4 uses these results to simulate the orbital evolution of individual real/fictitious satellites. The effects on satellite systems and possible restraints on planetary migration are discussed in Section 5. Last of all, conclusions close this manuscript in Section 6.

2. OUTLINES OF THE METHOD

The principal aim of this work is to analyze the perturbations of planetesimal fly-bys on satellite orbits. Then, as a first step, we need to know the distribution of these close encounters: their relative velocity, the type of motion relative to the planet, frequency, planetesimal mass, etc. This in turn implies that we must begin by simulating the planetary migration itself. In view of this, we divide our work into two parts:

- Simulation of planetary migration: Our first aim was to reproduce the results of classical studies of planetary migration such as, for example, Hahn and Malhotra (1999). We placed the four jovian planets amidst a disk of 1000 massless planetesimals distributed in a certain interval of semimajor axis and having a certain distribution of eccentricities and inclinations. The total number of planetesimals was determined by our CPU limitations. During the evolution of this system, we checked for planetary encounters, defined when the distance between a planetesimal and a planet was smaller than the distance $f \times R_{Hill}$, where R_{Hill} is the planetary Hill radius and f is a factor larger than unity. Each encounter was registered in detail, keeping track of the position and velocity of the planetesimal (in the planetocentric reference frame) throughout the passage. Since the disk was supposed massless, during this simulation the planets themselves did not migrate explicitly. The secular changes in the planetary orbits were later modeled by an "action–reaction" principle, through the changes in heliocentric energy and angular momentum (per unit mass) suffered by the planetesimal population.

- Effects of the encounters on satellite orbits: Having a database of all the encounters, we used this information as a starting ground for a second simulation. The idea now was to place a group of fictitious/real satellites (also considered as massless particles) orbiting each planet and take from the database of the previous simulation each encounter registered with that particular primary. Assigning a certain non-zero mass m to each planetesimal, we simulated the perturbative effects of the close approaches on the orbit of each of the satellites. Since this same value of m also yielded a certain value for the planetary migration, we hope to obtain a relationship between the stability of the satellite systems and the secular changes in the semimajor axes of the outer planets.

A word of caution at this point: During both simulations, we are representing the original planetesimal disk by a limited population of 1000 bodies. One may ask whether this approximation is adequate, and whether our results are expected to represent the effects of the original disk. The answer to this question depends on two aspects: (i) the mass distribution of the “real” residual disk after the formation of the planets, and (ii) the type of physical processes that dominate the dynamical evolution of the planets and satellites.

On the first point, it must be recalled that planetary formation in the outer Solar System is not yet well understood, and thus the final mass distribution is still an open problem. Perhaps one of the main questions is whether accretion proceeded in a classical runaway manner (Greenberg *et al.* 1978) or if it was dominated by an oligarchic growth (e.g., Ida and Makino 1993). In the first case, we would expect a population with very few large bodies and in which most of the total mass remained in small bodies in the 10- to 100-km-size range (Kokubo and Ida 1998). In the second scenario, runaway only occurred during the first stages of accretion, but stopped for each embryo after it reached a maximum size on the order of ≈ 1000 km. After this point, larger embryos grew slower than smaller ones, resulting in a (more or less) constant mass distribution for the large bodies. If the accretion timescales varied inversely proportional to the cube of the distance from the Sun, and since the Saturn core (approximately 10 Earth masses) formed at 9 AU, then it is quite conceivable that the final mass distribution at 10–35 AU contained several hundreds of Mars-size (or larger) bodies. Actually, it may be argued that numerous large bodies indeed formed in this part of the Solar System. For example, the large Uranus obliquity ($\approx 97^\circ$) may have originated in late stages of the accretion of this planet by massive planetesimals impacts (Lissauer and Safronov 1991, Slattery *et al.* 1992).

However, even if several hundred of Mars-size bodies are expected in the 10- to 35-AU region, it is still not clear whether they dominated the mass distribution of the residual disk. If this were the case, then our initial swarm of 1000 large bodies would be a fairly good representation. Nevertheless, this question is not fundamental for numerical simulations, as long as the dynamical evolution of the system is governed by physical processes which do not depend explicitly on the number of particles. Since planetary migration seems to be mainly due to the interplay of asymmetries in the planetesimal disk (e.g., Ida *et al.* 2000), a “real” disk of an excessively large number of planetesimals can be modeled by a population of 10^3 bodies with relative safety. Of course numerical noise is unavoidable, but the magnitude of the orbital migration depends fundamentally on the total mass of the disk and not on the number of bodies. For this reason, our results for the first part of the present work should be fairly reliable. The size–frequency distribution of planetesimals in a real disk becomes more crucial to the second part of the present work. We explain our approach to this issue in Section 4.2.

3. PLANETARY MIGRATION

3.1. Initial Conditions and Model

Our first integration was performed using the Swift RMVS3 integration code (Levison and Duncan 1994) and simulated the evolution of a disk of 1000 massless planetesimals subjected to the gravitational perturbations of the four major outer planets. The planetesimal swarm was distributed in the interval 10–40 AU with density $\propto a^{-1}$ (a being the semimajor axis). Initial eccentricities were taken as 0.01 and initial inclinations as half this value, thus simulating a cold disk. All angular variables were chosen randomly between zero and 360° . The massive planets were initially put in their hypothetical pre-migration positions. These initial conditions were obtained following the same approach used by Gomes (1997, 1998, 2000) and Levison *et al.* (2001), i.e., starting from the planetary present positions, a backward integration was performed applying a non-conservative force that simulates the migration in the opposite sense. In this way, the initial values of the semimajor axes were $a_{\text{Jup}} = 5.4$ AU, $a_{\text{Sat}} = 8.8$ AU, $a_{\text{Ura}} = 16.5$ AU, and $a_{\text{Nep}} = 23.0$ AU. Finally, the planetary masses were taken as their present values. We treated the planetesimals as massless particles; thus, the simulation was performed disregarding the gravitational perturbations of the swarm on the planets.

Total integration time was 10^7 years with a timestep of 0.17 years. The close encounters between planetesimals and planets were identified each time the planetocentric distance was smaller than $R_{\text{crit}} = 2R_{\text{Hill}}$. During the whole time interval the body remained inside a sphere of R_{crit} radius, the following information was registered: time, planet and planetesimal involved, planetocentric coordinates and velocities of the planetesimal, heliocentric energy and heliocentric angular momentum of the same body. This information was stored at fixed intervals Δt , which varied from 0.017 to 0.17 years, depending on which planet was involved in the encounter.

3.2. Results

We begin analyzing the encounters suffered by Jupiter. The two top plots in Fig. 1 show the cumulative number of close encounters as a function of time. $N(\text{ext})$ presents what we called “exterior” encounters and are defined by the condition that the planetocentric distance of the planetesimal r is smaller than $2R_{\text{Hill}}$. All passages with $r > 2R_{\text{Hill}}$ were not registered. This limit was chosen after several test runs and after checking that the effects of the neglected encounters were not significant to the migration process. The quantity $N(\text{int})$ shows the number of “interior” encounters, where $r < R_{\text{Hill}}$. We can see that both numbers grow rapidly and, although there appears to be an indication of a lowering of the steepness, we can see that after 10^7 years there is still a large number of encounters taking place. This seems to confirm the results of Hahn and Malhotra (1999), who predicted that the evaporation of the residual disk of planetesimals could not have taken less than 10^7 years, contrary to

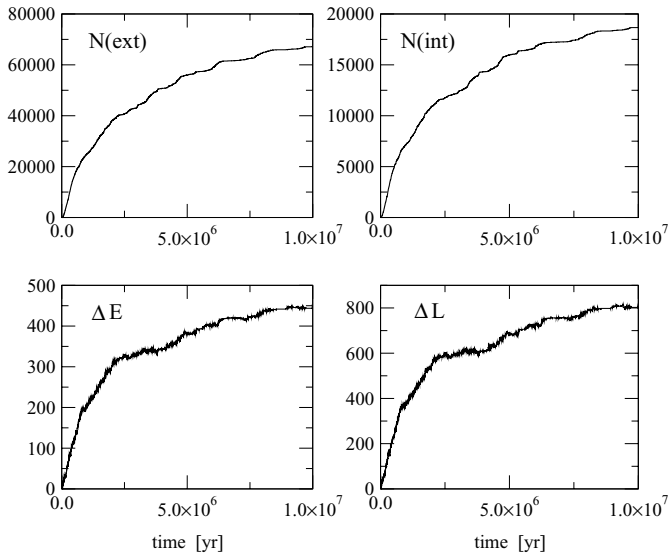


FIG. 1. Encounters with Jupiter. $N(\text{ext})$ denotes the cumulative number of exterior encounters (i.e., $r < 2R_{\text{Hill}}$) as a function of time. $N(\text{int})$ is the cumulative number of interior encounters (i.e., $r < R_{\text{Hill}}$) as a function of time. ΔE denotes the total change in heliocentric energy of the planetesimals, per unit mass, summed over all the encounters. ΔL is the total change in angular momentum.

other estimates such as those discussed in Fleming and Hamilton (2000).

The number of interior encounters follows practically the same trend as the exterior encounters, indicating that there seems to be no overall temporal change in the preference between both types. The ratio between both numbers is about 25%, and this remains more or less constant throughout the simulation. Moreover, this value is practically the same for all outer planets. This appears to indicate no significant gravitational focusing of the planets at $(1 - 2) \times R_{\text{Hill}}$ distances, plus a great isotropy in the encounters themselves, as seen from the planetocentric reference frame. This last property is due to the fact that our planetesimal disk is thick enough.

In the same figure, ΔE shows the temporal change in the heliocentric energy (per unit mass) of the planetesimals. It presents a monotonous trend toward positive values. This means that, on average, these bodies gain energy after close encounters with Jupiter. Thinking now on the consequent effect on the planet, this means that Jupiter itself loses energy as a function of time due to these same encounters. Since the total energy must be conserved, this implies that the change in orbital energy of the planet ΔE_P must be equal in magnitude but opposite in sign as the effects on the small bodies. Thus $\Delta E_P = -\Delta E$. Since loss of energy implies a decrease in semimajor axis, we can conclude that the value of a_{Jup} should manifest a decrease with time, exactly as found from previous works (e.g., Fernandez and Ip 1984). Finally, ΔL shows the change in angular momentum (per unit mass) of the planetesimals. It is possible to use these data to obtain the temporal variation of the eccentricity for each planet.

Figure 2 shows the cumulative ΔE_P (per unit mass) for all planets, as a function of time. In the case of Jupiter and Saturn, we can see that the trend is as expected from previous works, indicating a loss of energy for the first planet and a gain in energy for the second. The two outermost planets, however, do not show such a seemingly monotonic trend. For both the energy decreases during the beginning of the integration but then reverses itself after a couple of million years. The overall behavior, nevertheless, is adequate, once again indicating an outward migration for both massive bodies.

Let us recall that, since the planetesimals were considered massless, the integration did not yield explicit values for the migration of the planets. Nevertheless, we can use the classical swing-by formulation to relate the change of energy of the particles with the corresponding variation in semimajor axis of each planet. This is given by

$$a(t) = -\frac{1}{2}k^2 M_{\text{Sun}} \left(E_0 + \frac{m}{M_p} \Delta E(t) \right)^{-1}, \quad (1)$$

where k is Gauss' constant, M_{Sun} is the Solar mass, M_p is the mass of the planet, a_0 is its initial semimajor axis, and $E_0 = -k^2 M_{\text{Sun}} / 2a_0$ is its initial orbital energy. From the results in Fig. 2, it is possible to compute the variation in semimajor axis supposing certain values for the planetesimals' masses m . The value of m was chosen independently for each planet in such a way as to yield a planetary migration from the initial orbits to present values of a . Thus, for example, the value of m for those planetesimals having encounters with Jupiter was chosen such that the computed final semimajor axis is equal to 5.2 AU, similarly for the remaining planets. Results are shown in Fig. 3.

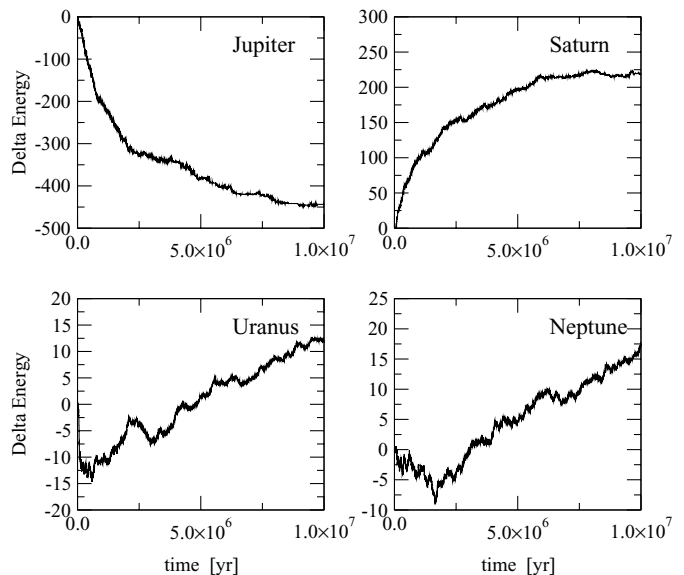


FIG. 2. Total change in heliocentric energy of the planetesimals, summed over all the encounters with the different planets.

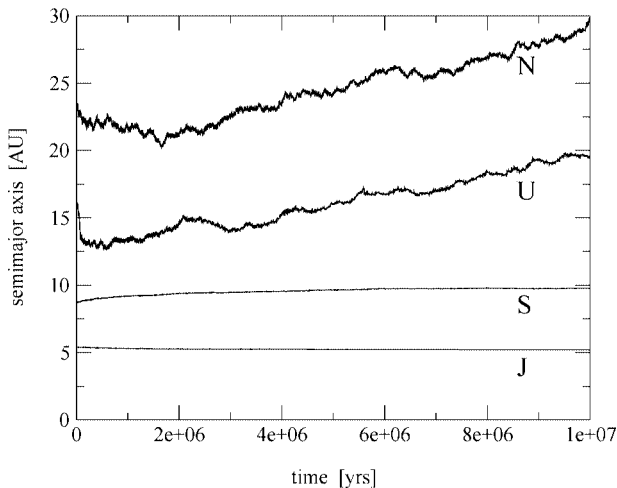


FIG. 3. Simulation of the migration in semimajor axis for all major outer planets.

The masses necessary for this are given below:

$$\begin{aligned}
 \text{Jupiter: } m &= m_0 \equiv 0.1M_{\oplus} \\
 \text{Saturn: } m &= m_0 \equiv 0.1M_{\oplus} \\
 \text{Uranus: } m &= m_0 \equiv 0.3M_{\oplus} \\
 \text{Neptune: } m &= m_0 \equiv 0.2M_{\oplus}.
 \end{aligned} \tag{2}$$

We note that they are not equal for each planet, so it appears as though different masses for the planetesimal disk are necessary to reproduce a migration to present orbits. This apparent inconsistency (or rather, incompatibility with results by Hahn and Malhotra (1999)) is due to the fact that in our simulation the planets do not migrate. This has the consequence that the outer part of our planetesimal disk (from approximately 28 AU onward) remained untouched and never experienced close encounters with any planet. This contrasts with a simulation where the outward motion of the planets constantly excites the orbits of the outer fringes of the disk and thus constantly renews the planetary feeding zones. Since this effect would be more noticeable for Neptune and Uranus than for the inner massive bodies, we need to increase (artificially) the mass of the outer planetesimals in our integration to counteract our approximations.

Supposing a constant mass of $m = 0.1M_{\oplus}$ for the whole population of planetesimals, the total mass for the disk is approximately 100 Earth masses. This value is about twice that proposed by Hahn and Malhotra (1999) for similar values of Jupiter’s migration. Nevertheless, we must note two things. First, our system was traced for 10^7 years, only one third of the integration time of this previous work. Second, since in our integration all particles with $a > 28$ AU did not participate in the process, this means that only about 625 planetesimals suffered at least one close approach. Consequently, the total mass of the “active” population was only about $63M_{\oplus}$, a value much more consistent with the Han and Malhotra simulation.

The greatest advantage of our scheme is the fact that the values of m can be modified after the integration is performed, and thus we obtain results for different simulated masses of the planetesimal disk without having to do further CPU-expensive calculations. Let us define a positive real parameter β as

$$\beta = \frac{m}{m_0}, \tag{3}$$

where m_0 is the planetesimals’ mass given by Eqs. (2), and m is a new different value. In the case of Neptune, for example, if we consider a value of $m = \beta \times 0.2M_{\oplus}$, we will obtain an orbital migration for the planet equal to $\Delta a_{Nep} = \beta \times 7.0$ AU. Thus, a value of $\beta = 0.5$ will yield a migration only half that predicted by Hahn and Malhotra. Similar considerations hold for the remaining planets as well. Since different values of β will also yield different perturbations on the planetary satellites (as will be discussed in Section 4), we can automatically relate instabilities in satellite systems with the corresponding magnitude of planetary migration.

As a final note, it is important to stress that the principal objective of this work is not to obtain a general and consistent model for the migration process. We are not particularly concerned with the migration timescales or total mass of the particle disk. Our aim is, however, to relate a given variation in semimajor axis of a planet with the perturbations on its satellite system. The use of our scheme allows us to efficiently sample the parameter space without additional simulations.

3.3. Analysis of the Planetary Encounters

The next step is to analyze the distribution of planetocentric orbits of the planetesimals. Typical questions we wish to address are: How close do the planetesimals get to the planet? Do they reach the region presently occupied by the satellites? What is the relative velocity at pericenter? What type of planetocentric orbits do they show? Do we find temporary captures?

As a first step, we approximated the close encounters with conics, computing the osculating planetocentric orbital elements at pericenter. Although this is not a good representation for planetary distances on the order of $2R_{Hill}$, the conics give an adequate approximation in the vicinity of the satellite region (i.e., <0.1 AU). Typical results are presented in Fig. 4 for planetary distances a few tenths of one Hill radius. Sample data points from the database are shown as crosses in a planetocentric non-rotating reference frame. The position of the planet (origin of the coordinate system) is denoted by a black circle. The two-body approximation is superposed to the crosses. Note that in some cases the best conic is not a hyperbola but an ellipse, denoting temporary captures of the planetesimals.

We can now assign to each encounter a given conic and use the orbital elements to estimate the minimum distance to the planet, maximum velocity, etc., and correlate this to other information, such as change in energy or angular momentum. We begin plotting the (planetocentric) eccentricity as a function of

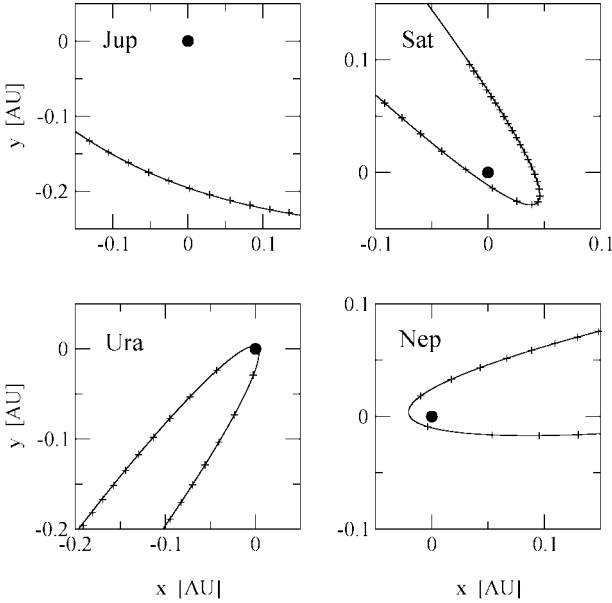


FIG. 4. Close encounters with each of the planets, as seen in the planetocentric (x, y) plane. Crosses indicate positions obtained from the database of the simulation. Lines represent a conic approximation of the orbit as determined with the position and velocities of the closest approach of the planetesimal to the planet. Black dots indicate the position of the primary.

(planetocentric) semimajor axis for every encounter with each planet. The results are shown in Fig. 5, where each dot corresponds to a single encounter. First, we can see that the number of elliptic ($e < 1$) encounters is small for Jupiter and Saturn, but this number grows significantly for the other planets. Very possibly, this is due to the fact that Uranus and Neptune are well immersed in the initial disk, so many planetesimals have close approaches with low relative velocities. Each distribution

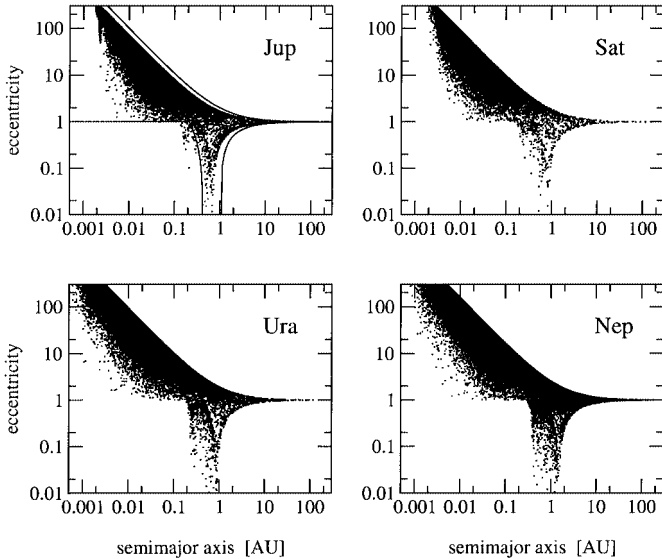


FIG. 5. Eccentricity vs semimajor axis for all encounters with each planet. Note that $e > 1$ denotes hyperbolic motion and $e < 1$ ellipses.

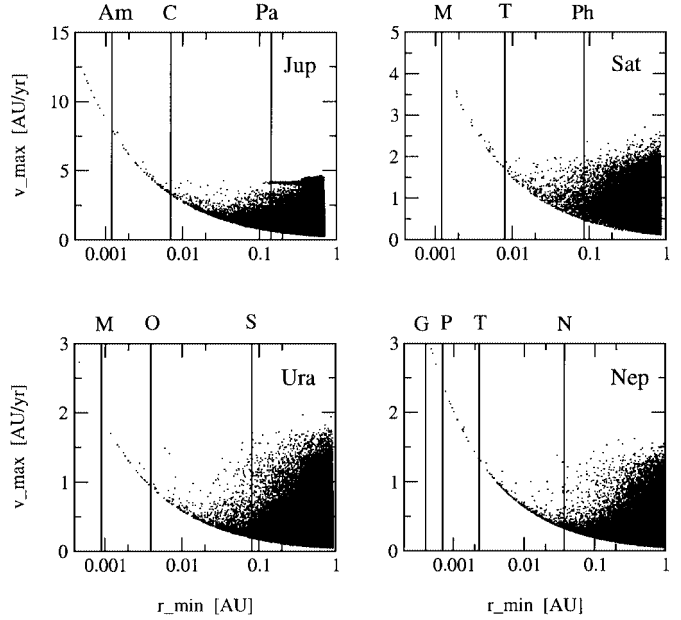


FIG. 6. Encounter velocity at pericenter (i.e., v_{max}) vs distance of closest approach (i.e., r_{min}). Vertical lines show the semimajor axis of representative bodies of each major group of real satellites around each planet. See text for details.

is delimited by three curves (seen in the graph for Jupiter). The two bounding the distribution at large a are given by the condition of elliptic orbits (bottom curve) and hyperbolic orbits (top curve) having pericentric distance to the planet less than $2R_{Hill}$. Finally, the curve at the bottom left is given by the condition that the pair (a, e) is such that the orbit is not bounded to the planet in the three-body approximation (Sun + planet + planetesimal). This is approximately given by the value of the Jacobi constant equal or larger to the value corresponding to the L_1 Lagrange point. Note that the actual distribution of points is very well encompassed within these bounds.

The next step is to use the orbital elements of the conic approximations to calculate minimum planetocentric distance and maximum planetocentric velocity and see what proportion of the encounters pass really close to the satellite systems. For the perturbations on the satellites to be even marginally significant, the passages have to be really close. Results are shown in Fig. 6. Vertical lines show the approximate semimajor axes for representative bodies of the main groups of satellites of each planet. On top of each line the satellite is indicated by letters. From left to right, each line corresponds to the following bodies:

- Jupiter: (Am) Amalthea, (C) Callisto, and (Pa) Pasiphae.
- Saturn: (M) Mimas, (T) Titan, and (Ph) Phoebe.
- Uranus: (M) Miranda, (O) Oberon, and (S) Sycorax.
- Neptune: (G) Galatea, (P) Proteus, (T) Triton, and (N) Nereid.

Figure 6 shows significant differences among the planets. For Jupiter and Saturn, both the retrograde and irregular satellites

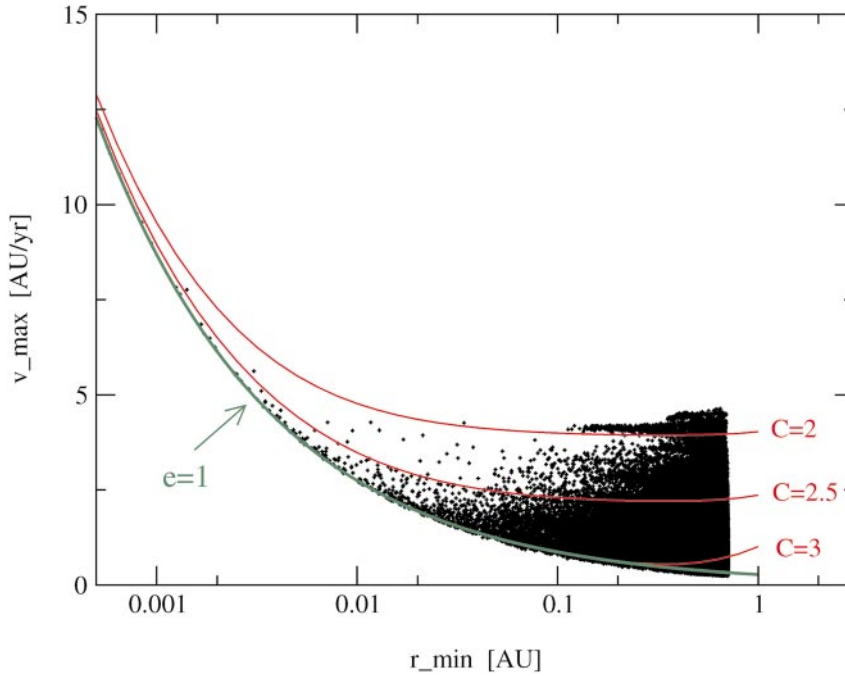


FIG. 7. Jupiter: Comparison of numerical data with curves of constant C . Top red line corresponds to $C = 1$, middle red line to $C = 2.5$, and bottom to $C = 3$. Green line marks parabolic orbits.

(rightmost vertical lines) seem to suffer many close passages. Regular and Galilean satellites suffer few encounters, and small inner bodies practically none. Moreover, these last encounters all happen at large relative velocities, so their effect should be very small. In the case of Uranus, only retrograde satellites have many encounters. Prograde irregular bodies very few, and inner bodies even less. The same is noted for Neptune.

Most of the encounters in Fig. 6 are located above a limiting curve. This curve is better observed in Fig. 7 (green line) and is given by

$$v^2 = \frac{2GM_p}{r}, \quad (4)$$

which defines an orbit as being parabolic. From Fig. 6 it is clear that, at smaller pericentric distances, the orbits tend to be more parabolic, while at larger pericentric distances we find a whole spectra of orbits, from elliptic to hyperbolic. This implies that the stability of satellites will be primarily affected by the quasi-parabolic encounters. This is not a surprising result. In fact, the encounters at small planetocentric distances are less affected by the solar tide, and the temporarily captured bodies are able to return to “infinity” only if they have the required energy, i.e., are quasi-parabolic. On the other hand, encounters at large planetocentric distances can have energies smaller or larger than parabolic, and the bodies will still be able to escape helped by the solar tide.

The above explanation has a rigorous proof in the conservation of the Jacobi constant C during the encounters. It is easy to show

that, for constant values of C , the relationship between v_{max} and r_{min} is given by

$$v_{max} = \frac{2\pi a_p}{T_p} \sqrt{(1 - \mu)^2 + 2(1 - \mu) + 2\frac{\mu}{r_{min}} - C}, \quad (5)$$

where $\mu = M_p / (M_{sun} + M_p)$, a_p is the semimajor axis of the planet, and T_p is its orbital period in years. For planet crossing orbits at heliocentric distances of 10–35 AU, typical values of C are in the range of 2–3. Figure 7 shows the results from Eq. (5) for three different values of C (red lines). It is clear from this figure that, at small pericentric distances, the curves $C = \text{const}$ tend asymptotically to the green curve, i.e., to parabolic orbits. The same result is obtained for the remaining three outer planets.

4. EFFECTS OF ENCOUNTERS ON SATELLITE ORBITS

We now have a dataset of all the close encounters suffered by each planet during the evolution of the planetesimal disk. Although in the first part of the present work these bodies were massless, we can now assign a mass to each of them and correlate the resulting planetary migration with the perturbations that each fly-by will induce on satellite orbits. Let us recall that we can define an external parameter $\beta = m/m_0$, where m is the assigned mass of each planetesimal (which can be varied freely), and m_0 would be the mass if we suppose a planetary migration as proposed by Hahn and Malhotra (1999) for a disk with mass equal to $50 M_\oplus$. For the time being, however, we will not try to directly relate possible instabilities of the satellites and the

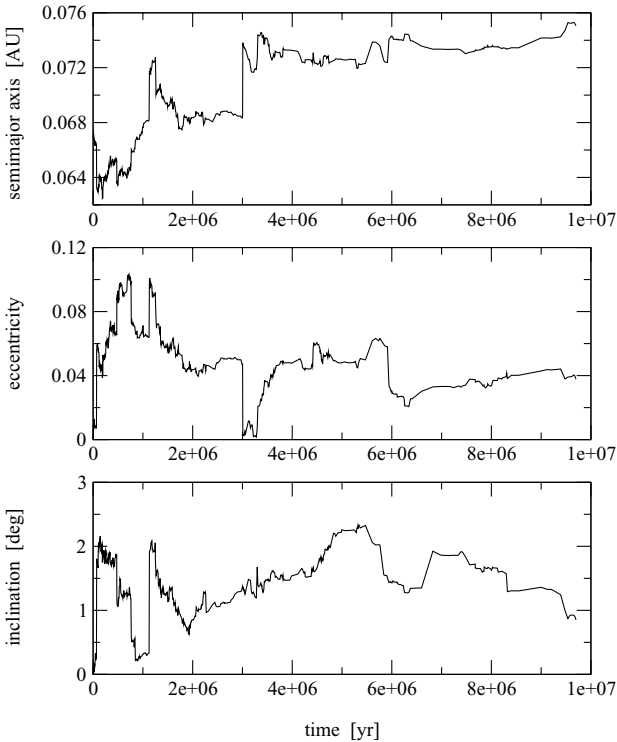


FIG. 8. Jupiter: $R_{Hill} = 0.355$ AU. Evolution of planetocentric semimajor axis, eccentricity, and ecliptical inclination for an initially planar circular satellite with $a = 10^7$ km $\simeq 0.067$ AU. Parameter β was taken equal to one.

planetary migration. This point will be discussed in the next section. For now, β is simply an indicator of the mass of each planetesimal, in units of some pre-defined m_0 .

For the simulations of this second part of our work, we used a specially designed code, based on subroutines of Swift RMVS3 (Levison and Duncan 1994). We assumed a massive planet to be the central body, with the satellites represented by a swarm of massless particles orbiting it. The passage of massive planetesimals during an encounter was simulated using the planetocentric coordinates already stored in the first part of our work. We used a two-body interpolation to get the position of the massive planetesimals at intermediate steps. Furthermore, the orbits of the satellites between encounters were supposed fixed and advanced using a two-body approximation. In other words, both solar perturbations and effects due to the oblateness of the central planet were neglected. This later approximation was necessary to keep the CPU time within reasonable limits. We performed several runs of groups of fictitious satellites at different distances around each of the jovian planets. In all cases, initial eccentricities and inclinations (with respect to the invariable plane of the outer Solar System) were taken as zero. The idea was to let the encounters themselves introduce any instabilities, without starting from elliptic or inclined orbits which would be easier to destabilize. The complete integration spanned 10^7 years, and the fixed timestep varied from 1 to 60 days, depending on the central planet under consideration and the average planetocentric

distance of the simulated satellites. The timestep was reduced by a factor of 100 whenever a satellite had a close encounter within 1 Hill radius to a planetesimal.

4.1. Examples of Single Satellites

In a first series of runs, and to see the general aspect of the behavior of the system, we took a single fictitious satellite around each planet. Its semimajor axis was taken $a = 10^7$ km $\simeq 0.067$ AU for Jupiter, Saturn, and Uranus, and $a = 5 \times 10^6$ km $\simeq 0.037$ AU for Neptune. In the case of Jupiter and Saturn, a satellite with $a \simeq 0.067$ AU roughly corresponds to the outer satellites. In the case of Uranus, this semimajor axis corresponds to the retrograde bodies. For Neptune, the initial condition corresponds approximately to Nereid's semimajor axis. Results for Jupiter and Neptune are shown in Figs. 8 and 9. The case of Saturn is analogous to Fig. 8 and is not shown. Similarly, the case of Uranus is analogous to Neptune. The value of β was set to $\beta = 1$ for Jupiter and Saturn, and $\beta = 0.25$ for Uranus and Neptune.

In the case of Jupiter's satellite (Fig. 8), we can see that the evolution of its orbit is significantly chaotic with several large-scale variations throughout the whole integration time. Each encounter induces a quasi-instantaneous change (at least in the

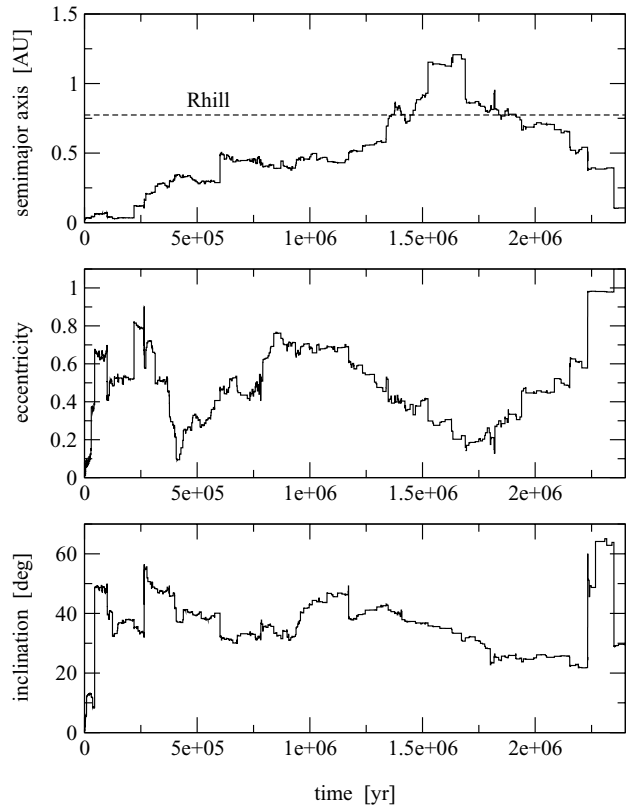


FIG. 9. Neptune: Evolution of planetocentric semimajor axis, eccentricity, and inclination for a fictitious satellite. Initial semimajor axis was taken as $a = 5 \times 10^6$ km $\simeq 0.037$ AU, which corresponds roughly with Nereid. Parameter $\beta = 0.25$.

scale of the plots) in the orbital energy and angular momentum of the satellite. According to the relative location of both bodies at the moment of closest approach, this change can be either positive or negative (Beaugé, in preparation). Since this geometry is different (and unrelated) for each successive passage, the resulting effect is similar to a random walk in each orbital element. In Fig. 8 the semimajor axis shows a significant overall secular increase, from 0.067 to about 0.076 AU. Although this does not in itself imply orbital instability, if other sufficiently massive satellites were put in its vicinity, their interactions could be significant, yielding possible mutual collisions. The present collisional lifetime of the retrograde satellite group of Jupiter is larger than 4 Gyr (Kessler 1981). Both the eccentricity and inclination also show a random-walk behavior. Nevertheless, their maximum value is never large. Thus, it seems that although the encounters can introduce some chaotic variations in the orbital elements of the satellite, there are no large-scale instabilities associated with these perturbations at $a \simeq 0.067$ AU.

Neptune's satellite (Fig. 9) shows a different behavior. Recall that the initial semimajor axis of this body is similar to that of the present Nereid. Moreover, in this case we chose $\beta = 0.25$. First, we also note a secular change in the semimajor axis, although this time the magnitude is much larger. Initially located at $a \approx 0.037$ AU, it reaches 1 Hill radius (indicated by the horizontal broken line) in about 1.3×10^6 years. According to Hunter (1967) and Nesvorný *et al.* (2002) when the value of a already reaches approximately $0.5 R_{Hill}$, a prograde satellite becomes unstable due to solar tides (for retrograde orbits, this limit is approximately $(0.7 - 0.8) \times R_{Hill}$). A large instability is also noted in the eccentricity. Initially zero, it rapidly reaches a value around 0.8 and then oscillates during the whole interval, until it finally reaches hyperbolic values at $t \approx 2.4 \times 10^6$ years. Even though this occurs much later than the time $a > R_{Hill}$, we must recall that our model does not include solar perturbations. Thus, the effects on the eccentricity are solely due to the encounters with planetesimals. Last of all, the inclination presents a more-or-less monotonic growth over the whole time interval, with a maximum value reaching about 50° . We can thus conclude that this body is in an extremely unstable region, and the perturbations due to the encounters cause its expulsion from the primary in a few million years.

These two results indicate large differences between the planets. While in the cases of Jupiter and Saturn, the encounters induced only small-scale orbital variations (even for $\beta = 1$), for Uranus and Neptune they quickly expelled the satellite from the system (even for $\beta = 0.25$). The reasons for this difference are twofold. First, the number of encounters suffered by the satellites of Uranus and Neptune are much larger than those suffered by Jupiter and Saturn. This is partially due to the fact that these latter planets were originally located below the inner border of the particle disk and thus received planetesimals only after they suffered several encounters with the outermost planets. However, this is also a consequence of the fact that Uranus and Neptune have a much smaller mass; thus planetesimals must

undergo repetitive encounters before crossing orbits are reached with Jupiter and/or Saturn.

The second reason is related to the relative planetocentric velocities of the planetesimals at the closest approaches. As was seen in Fig. 6, the encounters with Uranus and Neptune typically occur with v_{max} approximately half the value of those reaching Saturn, and about one quarter the value of those encountering Jupiter. Since the perturbative effects of each fly-by are proportional to the duration of the encounter, this means that a given encounter will induce larger perturbations in the satellite systems of the outermost planets. We can thus conclude that the effects of the encounters are very dependent on the satellite system in question. More importantly, any orbital instabilities should appear primarily in satellites of Uranus or Neptune.

4.2. Random Walk and the Mass Distribution of the Planetesimal Disk

The fact that the dynamical evolution of the satellites is given by a random walk of the orbital elements was verified with a series of additional numerical simulations. In each simulation, the number of planetesimals was artificially increased by cloning several times each of the encounters in the simulation with only 1000 planetesimals. As a result, we confirmed that the net change in the orbital elements of the fictitious satellites scaled inversely proportional to the square root of the number of bodies N . This means that the instabilities generated by the encounters depend not only on the adopted value of β , but also on the number of planetesimals in the disk. A larger mass for the disk will yield larger variations in the orbital elements of the perturbed body, but a larger population of planetesimals will imply a smaller dynamical effect, even if the total mass of the swarm is maintained constant.

To quantify the dependence of the dynamical evolution of satellites with these quantities, we will introduce the following variables. Let us denote by M_D the total mass of planetesimals encountering a given planet. Call M_{D_0} the value such that $\beta = 1$ and planetary migration acquire the nominal magnitude. Thus, we can also write $\beta = M_D/M_{D_0}$. Furthermore, let us define \bar{m} as the principal (or dominating) planetesimal mass in the rocky disk. In our simulation, we determine the effect of the fly-bys on satellite orbits assuming a planetesimal mass of $0.1M_\oplus$. If other values are considered, it can easily be shown that this effect scales as

$$\alpha = \beta \sqrt{\frac{\bar{m}}{0.1M_\oplus}}. \quad (6)$$

Thus, if we consider that the mass of the residual planetesimal disk was dominated by large Mars-size bodies, $\alpha = \beta$ and any instabilities detected in our simulations will be a function solely of the adopted planetary migration. If, on the other hand, we have $\alpha = 0.25$, this can represent either a planetary migration of one quarter of nominal magnitude or a full migration ($\beta = 1$) but a planetesimal disk where the average mass of the population

was only about $\bar{m} \approx 0.005M_{\oplus}$. This is on the same order as the mass of Pluto.

5. SIMULATIONS OF COMPLETE SATELLITE SYSTEMS

The next step is to analyze the orbital variations of a large set of fictitious satellites, with initial semimajor axis chosen to cover the whole spectra of the real satellites. For each planet we took eight values of a in the interval $[0.0003, 0.13]$ AU. The lowest limit corresponds roughly to the inner groups of bodies; the highest limit to retrograde orbits for Jupiter, Saturn, and Uranus. For each value of semimajor axis we took 100 different satellites, each with initial circular–planar orbits (with respect to the invariable plane of the outer Solar System) but with mean anomaly M distributed uniformly from 0° to 360° . All satellites were taken massless, and their orbits were simulated considering the effects of all the encounters suffered by each planet. The value of α was taken equal to 0.25, 0.5, and 1.0 in different runs. For all satellites, we registered the complete temporal variation of semimajor axis, eccentricity, and inclination. A body was considered ejected from the system whenever it reached a pericentric distance smaller than the planetary radius or $e = 1$ and was deactivated from the simulation. We also computed the maximum, minimum, and mean final values of the orbital elements at $t = 10^7$ years. Mean values were determined by averaging over all the bodies with the same initial a that remained bounded to the primary.

5.1. Uranus and Neptune

We begin by analyzing the number of satellites, out of the initial 100 with the same a , that were deactivated from the simulation. This is shown in Fig. 10 for Uranus and Neptune, as a function of the initial radial distance and for three different values of α . Continuous lines indicate results for $\alpha = 1$, broken lines for $\alpha = 0.5$, and dotted lines for $\alpha = 0.25$. In the left-hand side plot, the present locations of the inner, central, and retro-

grade groups of uranian satellites are represented by Miranda, Oberon, and Sycorax, respectively, and are indicated by the letters M, O, S. In the right-hand plot, letters G, P, T, N show the positions of Galatea, Proteus, Triton, and Nereid.

For Neptune’s system, we can see that the perturbations due to the passages of the planetesimals are very destructive, even for very small values of the semimajor axis. For $\alpha = 1$ all test satellites with initial conditions similar to Nereid (and beyond) are ejected from the system (hyperbolic orbits or collisions with the planet). Although some test satellites survive for smaller distances to the planet, still approximately 70% of all fictitious bodies in the inner group (represented by Galatea) are also expelled.

The broken curve shows results supposing $\alpha = 0.5$. The region around and beyond Nereid is still sufficiently unstable so as to eject all bodies originally in this location. The region closer to the planet is still fairly unstable, even though not so marked as in the case $\alpha = 1$. Approximately 75% of the inner test satellites survive the integration, while only about half the Triton-type bodies end up still bound to the system. Finally, the dotted line presents results for $\alpha = 0.25$. We note that the instabilities are now significantly reduced. It is still observed that all satellites with $a > 0.1$ AU escape; however, the region around Nereid now shows over 25% of survivors. Test satellites with initial semimajor axis around Triton and smaller also show greater stability. Still, in all cases over a quarter of the original population escapes.

The plot for Uranus (Fig. 10, left) shows similar results. Once again the region presently occupied by the retrograde group (represented by Sycorax) is highly unstable for values of $\alpha > 0.25$. However, both the inner and central groups (represented by Miranda and Oberon) show lower instabilities than in Neptune’s case, indicating that this system is at least marginally more robust. For $\alpha = 1$, most of the test inner satellites survive the entire simulation.

The next question we wish to address is the final eccentricity distribution of those bodies which survived. This is shown in Fig. 11 for Uranus and Neptune as function of the initial semimajor axis. Top graphs correspond to $\alpha = 0.5$ and bottom plots to $\alpha = 0.25$. The continuous lines represent the mean final eccentricity $\langle e \rangle$, averaged over the bodies which remained bounded to the primary. The broken lines above and below represent the maximum and minimum values of the final eccentricity (i.e., e_{max} and e_{min}). Together, these three curves give a general idea of the dispersion of the final orbits. The shaded areas to the right of each plot mark the region where ejection was 100% efficient. Finally, the full circles denote the present orbits of the real satellites around each planet.

Both Nereid and Uranus’ retrograde satellites lie within the region of extreme instability. The inner and central satellites have final eccentricities which reach very high values (on the order of 0.2). Even though this in itself does not imply ejection or planetary impact, it puts them in mutual crossing orbits. Figures 11c and 11d, obtained with $\alpha = 0.25$ show a better agreement with

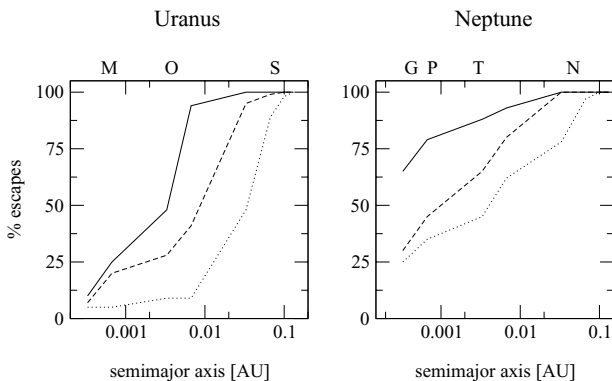


FIG. 10. Percentage of escaped satellites, as function of initial semimajor axis, for Uranus and Neptune. Continuous lines: $\alpha = 1$, broken lines: $\alpha = 0.5$, and finally, dotted lines: $\alpha = 0.25$.

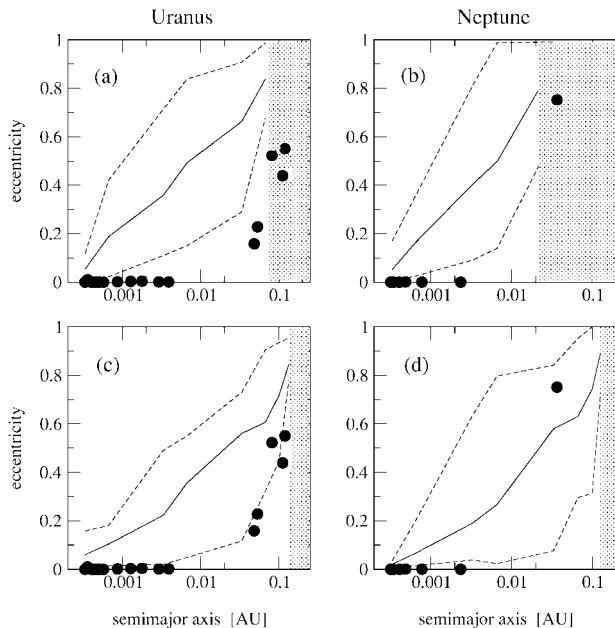


FIG. 11. Maximum, mean, and minimum eccentricity as a function of semimajor axis, for test satellites of Uranus and Neptune, and for $\alpha = 0.25$ and $\alpha = 0.50$. Black circles denote the present orbits of the real satellites. Shaded region on the right corresponds to the region for which 100% of the initial conditions were ejected or collided with the planet.

the observed distribution of satellites. Note that the present eccentricity of Nereid lies conveniently between the predicted values of e_{min} and e_{max} . This implies that even if this body originated in a circular orbit at the beginning of the migration, its present ellipticity could be explained by these perturbations. This would give an alternative explanation to that suggested by Goldreich *et al.* (1989), independent of hypothetical perturbations by Triton.

In the case of Uranus, Fig. 11c shows that the retrograde bodies have orbital eccentricities compatible with the values pumped by the encounters when $\alpha = 0.25$. In fact, the lower broken line follows the observed dependence of e with semimajor axis for the distant satellites of this planet. More importantly, the shaded region corresponding to extreme instability now lies beyond the upper limit of known satellites. We can therefore conclude that the present distribution of bodies around both the outermost planets seems to be much more compatible with a low value of α , unless the satellites were formed by the end of the migration process.

5.2. Jupiter and Saturn

As was expected from simulations of individual bodies, the effects of the encounters on satellite systems of Jupiter and Saturn are much less important. Even the case $\alpha = 1$ does not induce any significant number of escapes. All our test satellites remained bounded to the primaries, even for values of the semimajor axis as large as $a = 0.13$ AU (approximately $0.3R_{Hill}$). Figure 12 shows the final eccentricities of test satellites for both

planets. Analogous to Fig. 11, continuous lines indicate $\langle e \rangle$, while the broken lines show the maximum and minimum values of final e . For comparison, full circles show the present observed eccentricities and semimajor axes of the real satellites.

We note that although no escapes or planetary impacts were detected in the swarms, the increase of eccentricities is significant, especially for larger distances from the primary. This result (already seen in Fig. 11 for Uranus and Neptune) is due to two reasons. First, satellites with larger values of a are less bounded to the system and, thus, more easily perturbed. Second, as shown in Fig. 6, the number of close encounters increases with the planetocentric distance. Both effects contribute to the trend observed in Fig. 12. It is interesting to observe that the value of $\langle e \rangle$ at the region of distant satellites is very similar to that of the observed satellites.

The pumped values of e in the inner and central satellite regions tell two different stories. For Jupiter, these values are fairly small, with $\langle e \rangle$ never exceeding 0.05, and even e_{max} remaining limited by 0.1. Thus it seems that all these satellites, including the Galilean group, should not be greatly disturbed by the planetary migration, no matter how large. For the Saturn satellites, however, the excitation of peculiar velocities is a bit larger. Although the inner group is also relatively stable, the central region (i.e., $a \approx 0.01$ AU) has a mean eccentricity of about 0.1 with a maximum reaching 0.4.

5.3. The Effects on the Inclinations

Before analyzing the evolution of the satellites' inclinations due to the encounters, we would like to study the sensitivity of our results with respect to the reference plane chosen for these inclinations. In other words, all simulations presented in the previous sections were made by choosing satellite orbits which were initially planar with respect to the invariable plane of the outer Solar System. Since the obliquity of the planets is not in the least negligible, these initial conditions do not have any correspondence with planar orbits with respect to each planet's equator. So, it is important to see whether different initial inclinations yield different evolutions. To avoid confusion,

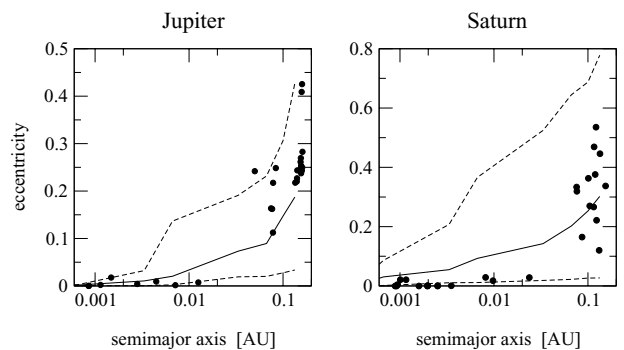


FIG. 12. Maximum, mean, and minimum final eccentricities as a function of the initial semimajor axis for test satellites of Jupiter and Saturn, using $\alpha = 1$. Black circles denote the present orbits of the real satellites.

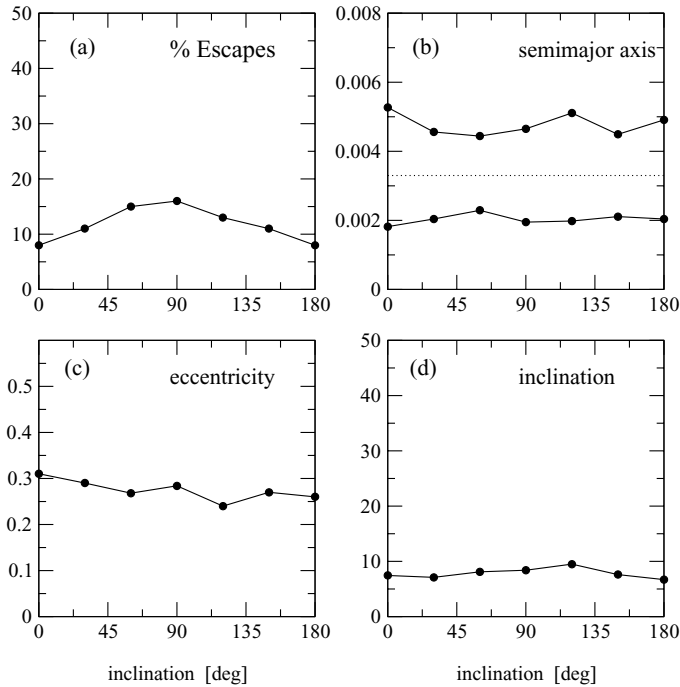


FIG. 13. Variation of the effects of the encounters are function of the initial inclination (I) with respect to the invariable plane. (a) Percentage of initial bodies that were ejected from the system. (b) Dotted line shows initial semimajor axis, while black circles indicate average apocentric distance (upper set) and average pericentric distance (lower set). (c) Average final eccentricity (e). (d) Average final change in inclination.

we will denote the satellite’s inclination with respect to the invariable plane by I and that with respect to the planet’s equator by i .

To test the dependence of the results on the inclination, we performed six sets of numerical simulations of swarms of 100 fictitious satellites in circular orbits around Uranus. The initial semimajor axes for all satellites were taken equal to 5×10^5 km (≈ 0.0033 AU). These initial orbits were chosen to be sufficiently stable to avoid a large proportion of ejected bodies but still show appreciable dynamical evolution for $\alpha = 0.25$. Each swarm varied by the inclination of its population with respect to the invariable plane; the initial values were taken equal to $n \times 30^\circ$ with $n \in [0, 6]$. For each swarm, we determined the number of escaped bodies and final average orbital elements of the surviving satellites. Results are shown in Fig. 13. We can see very little difference as a function of the initial I . Even though a certain dispersion is noted, there is no overall large-scale variation of the results.

Nevertheless, there are differences. For example, we note that the percentage of removed satellites (top left) is larger for bodies outside the invariable plane than those initially with $I = 0$. However, the remaining graphs do not show any significant differences in the final average values of the orbital elements. The main consequence of this observation is that if a fictitious satellite is initially placed in a planar orbit ($I = 0$) and its final inclination

is given by I_f then, on average, any other body placed with a different initial inclination $I_0 \neq 0$ should have a final value equal to approximately $I_0 \pm I_f$. Thus, the quantity I_f is a fairly good indicator of the evolution of the inclination of a satellite’s orbit, regardless of the plane with respect to which this inclination is measured. In particular, independent of the planet’s obliquity, there is little difference in placing a satellite in the equatorial plane (i.e., $i = 0$) or in the invariable plane (i.e., $I = 0$). Since it can be shown that there is no observed greater abundance of direct to retrograde encounters, there should also be no greater stability of retrograde satellites with regard to direct bodies. In this regard, perturbations due to close passages are more democratic than those coming from solar effects (Nesvorný *et al.* 2002).

With this in mind, Fig. 14 now presents the final averaged inclinations for the same swarms of fictitious satellites discussed in previous sections. In the case of Uranus and Neptune (Figs. 14c and 14d), the different curves correspond to $\alpha = 1, 0.5$, and 0.25 (see caption). Full symbols indicate the observed inclinations of those real satellites in direct orbits. Empty symbols show the retrograde satellites. In the latter case, the value of the inclination was plotted as $|180^\circ - I|$. For inner bodies, inclinations are measured with respect to the planet’s equator; for outer and retrograde, these are measured with respect to the Laplace plane.

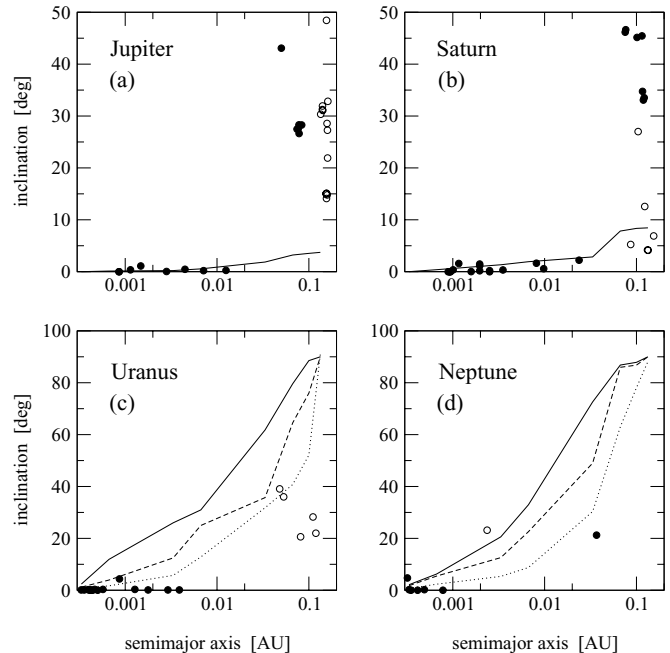


FIG. 14. Average final inclination of each swarm of fictitious satellites, as a function of the initial semimajor axis. Full symbols mark present inclinations of real bodies in direct orbits. Empty symbols show real retrograde satellites ($|180^\circ - I|$). For inner bodies, inclinations are measured with respect to the planet’s equator; for distant satellites, these are measured with respect to the Laplacian plane. Continuous lines correspond to $\alpha = 1$, broken lines to $\alpha = 0.5$, and dotted lines to $\alpha = 0.25$.

We can see no large-scale orbital variation in the case of the Jupiter and Saturn systems. Inner and central bodies remain practically in the plane and the final inclinations do not exceed $\approx 3^\circ$. Even in the retrograde region, the induced inclination jumps are smaller than 10° , showing that if these bodies are in fact captures, their original tilt with respect to the planet's equator should not have varied significantly. The cases of Uranus and Neptune are, as usual, more drastic. The excitation in inclination grows from very small values (close to the primary) to almost 90° for $a = 0.1$ AU.

5.4. The Inner Satellite Group

Until now we have mainly discussed the stability (or lack of it) through the increase in the eccentricity of initially circular orbits. We have seen that the outer and retrograde satellite groups are the most affected by the perturbations of the planetesimals' encounters and, in the case of Uranus and Neptune, the satellites have much difficulty surviving if the value of α is larger than 0.25. However, if several satellites are present in nearby orbits, then it is not necessary for their eccentricity to reach parabolic values for the group to be unstable. If the orbits are quasi-planar and/or the masses sufficiently large, the system will be unstable provided the pericentric distance q of the outermost body is smaller than the apocentric distance Q of the innermost satellite, as long as there are no mean motion resonances between them. Thus, in multiple satellite systems, bodies S_1 and S_2 on initially circular orbits, with semimajor axes $a_1 < a_2$, can be considered potentially unstable if

$$(a_1 + \Delta a_1)(1 + e_1) > (a_2 - \Delta a_2)(1 - e_2), \quad (7)$$

where e_i are the final eccentricities and $\Delta a_i > 0$ are the orbital changes in semimajor axis induced by the encounters with the planetesimals. Notice that this condition is much more subtle than simply requiring $e_i > 1$ and thus should be a much better indicator of the stability of the inner groups of satellites of the outer planets.

Figure 15 shows planetary distance versus semimajor axis for Uranus and Neptune's satellites, and for two different values of α . Black circles mark the position of the real satellites. For Uranus, letters M, A, U, T, O denote the locations of Miranda, Ariel, Umbriel, Titania, and Oberon. For Neptune, letters P and T correspond to Proteus and Triton. The dotted line is the identity function. The continuous curves above and below this line represent the average induced apocentric distance, $\bar{Q}(a)$, and the average induced pericentric distance, $\bar{q}(a)$, respectively. These quantities are defined as

$$\begin{aligned} \bar{q} &= (a - \Delta a)(1 - \langle e \rangle) \\ \bar{Q} &= (a + \Delta a)(1 + \langle e \rangle), \end{aligned} \quad (8)$$

where Δa is the final variation in semimajor axis, and $\langle e \rangle$ the average final eccentricity for satellites with the same initial a . Thus, any satellite with a given initial a will exhibit planetocentric ra-

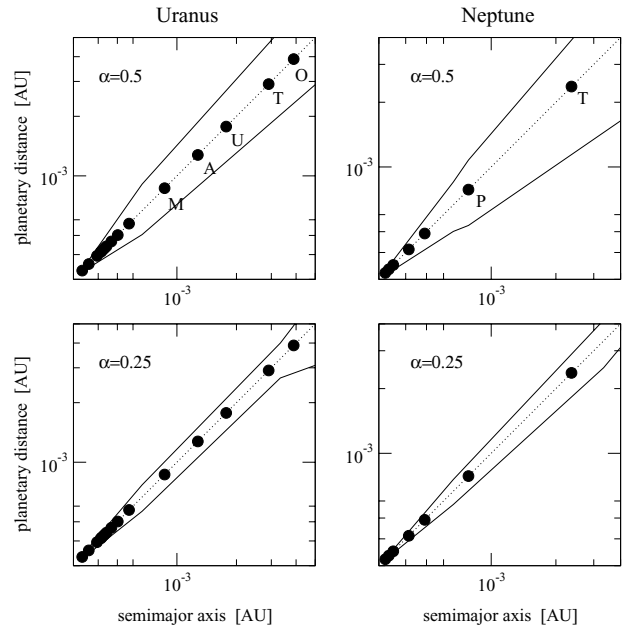


FIG. 15. Averaged induced pericentric and apocentric distances as a function of semimajor axis, for Uranus and Neptune. Black circles denote real satellites (see text for details). Top graphs are constructed with $\alpha = 0.5$, bottom plots with $\alpha = 0.25$.

dial incursions more or less delimited by the continuous lines in Fig. 15. This implies that any two satellites with initially $a_1 < a_2$ will be unstable due to mutual perturbations if $\bar{Q}(a_1) \geq \bar{q}(a_2)$, and they will be stable otherwise. It is worth recalling that this stability criterion is not rigorous, and the satellites may coexist in overlapping orbits provided: (i) their masses are very small, (ii) their mutual inclinations are large, or (iii) there exist a mean motion commensurability between them.

For $\alpha = 0.5$ (Fig. 15, top graphs) we note that the present distribution of real satellites does not seem to satisfy this condition for stability. This is clear from the results for Uranus, although only marginally for Neptune. In the former case, all the satellites overlap the orbits of those with similar a . For Neptune, however, things are not so evident. Proteus has an induced apocentric distance which is practically equal to the pericentric distance of Triton, but the overlap is marginal. The two bottom plots show the same results, only now for $\alpha = 0.25$. We can see that the radial incursions in this case are much more restricted, and the present sequence of semimajor axes of the Neptune satellites have a separation which is very stable. For Uranus, however, even in this plot the stability seems compromised, especially for the pair Titania–Oberon whose orbits still overlap. Nevertheless, we must remember that they were also significantly affected by tidal effects from the primary (e.g., Dermott *et al.* 1988) so their original separation in semimajor axes could have been much different in the past.

As an example, Fig. 16 shows the evolution of three fictitious satellites with initial semimajor axes similar to Miranda, Ariel, and Umbriel. The value of α was taken equal to 0.35. The shaded

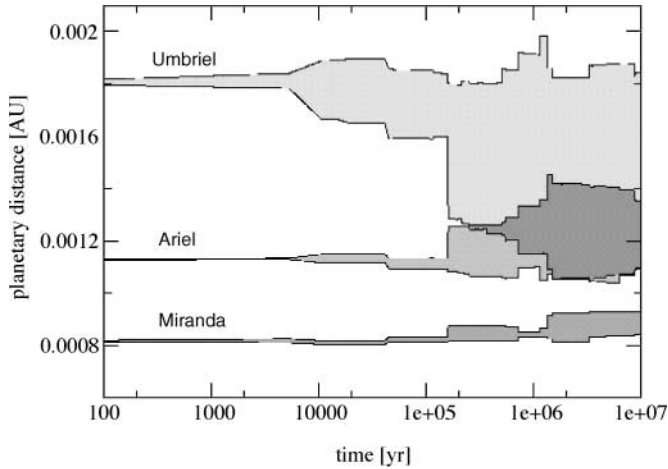


FIG. 16. Numerical simulation of fictitious satellites ($\alpha = 0.35$) with initial conditions similar to Miranda, Ariel, and Umbriel of the Neptune system. The shaded areas of each body mark the region with instantaneous planetary distance between $a(1 - e)$ and $a(1 + e)$. Note the overlapping of orbits for both exterior satellites at $t > 10^5$ years.

area of each body indicates the region of planetary distances inside the range $r \in [a(1 - e), a(1 + e)]$. Note that the orbits of the two outermost satellites start to overlap after 10^5 years.

So, once again we have evidence that values of $\alpha > 0.25$ would induce perturbations too large to be compatible with the observed inner satellite systems. This is important because we are now treating bodies whose primordial origin from the circumplanetary disk is fairly certain. Thus, unlike the outer and retrograde bodies, there is little doubt that these satellites were present during the whole process of planetary migration and evaporation of the residual rocky disk.

Finally, a similar analysis for the Jupiter and Saturn inner systems show very little radial incursions of the real satellites, and even for $\alpha = 1$ there is no observed overlap in the orbits of adjacent satellites. Thus, once again we note that these groups are extremely stable. This confirms our previous results (Section 5.2) in the sense that both these planets are massive enough to protect their satellites from external perturbations originating from even large values of α .

6. CONCLUSIONS

In this paper we have discussed the stability and orbital evolution of satellite systems of the major planets under the perturbative effects of close encounters with massive planetesimals. The dynamical characteristics of these encounters were obtained from a numerical integration in which we simulated the post-formation planetary migration due to the scattering of the residual disk material by the already formed planets (Fernández and Ip 1984). By assigning different masses to these planetesimals, we were able to relate different magnitudes of the secular variation in the semimajor axes of the planets (defined by a coefficient

β) with the gravitational perturbations of the planetesimals on fictitious planetary satellites.

Nevertheless, we found that the dynamical evolution of these fictitious bodies corresponds to a random walk in the orbital element space. As such, the magnitude of the net variation of the orbits is a function not only of β , but also of the dominant planetesimal mass in the original disk \bar{m} . Thus, although the perturbations of the fly-bys scale with β , their effects are proportional to a new parameter $\alpha = \beta\sqrt{\bar{m}/0.1M_{\oplus}}$.

If we assume that the large-body component (composed of Mars-size bodies) dominated the mass of the residual disk, then our results seem to indicate that the presently accepted change in the orbits of Uranus ($\Delta a_{Ura} \approx 3$ AU) and Neptune ($\Delta a_{Nep} \approx 7$ AU) is too large and are not compatible with the observed distribution of satellites if they were formed/captured before the migration began. In fact, even half this orbital change already causes sufficient instabilities to eject all the outer and retrograde satellites (including Nereid), plus originating mutual encounters between the inner satellite groups of both planets. Nevertheless, the real bodies are consistent with a migration whose magnitude only spanned one quarter of this value (i.e., $\Delta a_{Ura} \approx 0.7$ AU and $\Delta a_{Nep} \approx 1.7$ AU). Notwithstanding these results, the Jupiter and Saturn systems are not so susceptible to perturbations from passing planetesimals. Since the satellites are located deeper in the energy well, and the number of encounters is much smaller than for the outermost planets, practically all the simulated bodies remained in stable orbits.

On the other hand, if the real value of \bar{m} was much smaller than $0.1M_{\oplus}$, then larger magnitudes of migration are possible. However, even if the disk was made up of bodies of 1000-km size, nominal migration still implies values of $\alpha \approx 0.2$. It is interesting to note that such a value for Uranus and Neptune is not only consistent with the present distribution of satellites but also may help to explain some of their orbital characteristics. For Uranus, the eccentricities and inclinations of the irregular satellites show a good agreement with the values induced by the encounters, supposing initial circular and planar orbits. A similar result is noted for Nereid. The perturbations generated by this migration could be sufficient to excite an initially circular and planar Nereid to its present orbit, thus giving an alternative explanation for the origin of this body's dynamics, different from the scenario proposed by Goldreich *et al.* (1989).

The parameter α can also have a different interpretation. Imagine that the residual disk had a very marked bimodal mass distribution, which consisted in a very large quantity of very small bodies (e.g., 1- to 10-km size) and a number N_{mars} of Mars-size planetesimals. Although both populations contributed equally to planetary migration, the instabilities of the satellite systems was mainly determined by the fly-bys of the large-size bodies. Thus, in the case $\beta = 1$, and even if $\bar{m} \ll 0.1M_{\oplus}$, the parameter α can be written as

$$\alpha = \sqrt{\frac{N_{mars}}{1000}}. \quad (9)$$

With such a relationship, we obtain that a value of $\alpha = 0.25$ corresponds to $N_{mars} \approx 60$. This means that even if the original disk was dominated by small bodies, a relatively small number of Mars-size planetesimals could have introduced significant instabilities in the satellite systems of the outer planets. Consequently, even in the case $\bar{m} \ll 0.1M_{\oplus}$, the results presented in this paper may still be valid and could very well yield valuable constraints on the end product of the planetary formation process and/or alternative explanations for the present dynamical structure of several of the irregular satellites of the outer planets.

Last of all, we must recall that our model is approximate. We have not included the solar perturbations or oblateness effects in the evolution of the satellites. Furthermore, the dynamics of the planetesimals, the migration of the planets, and the evolution of the satellites were all treated independently and not in a self-consistent manner. However, it is important to point out that this paper is essentially exploratory in nature and, thus, certain assumptions and approximations are unavoidable. We have for the first time explored the stability of satellites in the early Solar System and used it to constrain the large-size component of planetesimals at 10–35 AU and/or the magnitude of planetary migration. We wonder whether more elaborate models and future research will confirm or negate our findings.

ACKNOWLEDGMENTS

The authors acknowledge support from the São Paulo State Science Foundation, FAPESP (Proc. 00/07084-0), the Brazilian National Science Council, CNPq (Proc. 300953/01-1 and 150085/01-0), and NSF Grant “Dynamical Studies of Planetary Satellites.” We are also grateful for numerous comments by G. Valsecchi and an anonymous referee, both of whom helped to greatly improve this work.

REFERENCES

- Brown, M. E., C. D. Koresko, and G. A. Blake 1998. Detection of water ice on Nereid. *Astrophys. J.* **508**, L175–L176.
- Bryden, G., D. N. C. Lin, and S. Ida 2000. Protoplanetary formation. I. Neptune. *Astrophys. J.* **544**, 481–495.
- Colombo, G., and F. A. Franklin 1971. On the formation of the outer satellite groups of Jupiter. *Icarus* **15**, 186–189.
- Dermott, S. F., R. Malhotra, and C. D. Murray 1988. Dynamics of the uranian and saturnian satellite systems—A chaotic route to melting miranda? *Icarus* **76**, 295–334.
- Duncan, M. J., H. F. Levison, and S. M. Budd 1995. The dynamical structure of the Kuiper Belt. *Astron. J.* **110**, 3073–3081.
- Fernández, J. A., and W.-H. Ip 1984. Some dynamical aspects of the accretion of Uranus and Neptune—The exchange of orbital angular momentum with planetesimals. *Icarus* **58**, 109–120.
- Fleming, H. J., and D. P. Hamilton 2001. On the origin of the Trojan asteroids: Effects of Jupiter’s mass accretion and radial migration. *Icarus* **148**, 479–493, doi: 10.1006/icar.2000. 6523.
- Gladman, B., J. J. Kavelaars, M. Holman, P. D. Nicholson, J. A. Burns, C. W. Hergenrother, J. M. Petit, B. G. Marsden, R. Jacobson, W. Gray, and T. Grav 2001. Discovery of 12 satellites of Saturn exhibiting orbital clustering. *Nature* **412**, 163–166.
- Goldreich, P., N. Murray, P. Y. Longaretti, and D. Banfield 1989. Neptune’s story. *Science* **245**, 500–504.
- Gomes, R. 1997. Dynamical effects of planetary migration on the primordial asteroid belt. *Astron. J.* **114**, 396–401.
- Gomes, R. 1998. Dynamical effects of planetary migration on primordial Trojan-type asteroids. *Astron. J.* **116**, 2590–2597.
- Gomes, R. 2000. Planetary migration and plutino orbital inclinations. *Astron. J.* **120**, 2695–2707.
- Greenberg, R., J. Walker, C. R. Chapman, and W. K. Hartman 1978. Planetesimals to planets. Numerical simulations of collisional evolution. *Icarus* **35**, 1–26.
- Hahn, J. M., and R. Malhotra 1999. Orbital evolution of planets embedded in a planetesimal disk. *Astron. J.* **117**, 3041–3053.
- Heppenheimer, T. A., and C. Porco 1977. New contributions to the problem of capture. *Icarus* **30**, 385–401.
- Holman, M. 1997. A possible long-lived belt of objects between Uranus and Neptune. *Nature* **387**, 785–788.
- Hunter, R. B. 1967. Motions of satellites and asteroids under the influence of Jupiter and the Sun—I. Stable and unstable orbits. *Mon. Not. R. Astron. Soc.* **136**, 345–265.
- Ida, S., G. Bryden, D. N. C. Lin, and H. Tanaka 2000. Orbital migration of Neptune and orbital distribution of trans-neptunian objects. *Astrophys. J.* **534**, 428–445.
- Ida, S., and J. Makino 1993. Scattering of planetesimals by a protoplanet: Slow-down of runaway growth. *Icarus* **106**, 210–227.
- Kessler, D. J. 1981. Derivation of the collision probability between orbiting objects. The lifetimes of Jupiter’s outer moons. *Icarus* **48**, 39–48.
- Kokubo, E., and S. Ida 1998. Oligarchic growth of protoplanets. *Icarus* **131**, 171–178.
- Levison, H. F., and M. J. Duncan 1994. The long-term dynamical behavior of short-period comets. *Icarus* **108**, 18–36.
- Levison, H. F., L. Dones, C. Chapman, S. A. Stern, M. J. Duncan, and K. Zahnle 2001. Could the lunar “late heavy bombardment” have been triggered by the formation of Uranus and Neptune? *Icarus* **151**, 286–306.
- Lissauer, J. J., and V. S. Safronov 1991. The random component of planetary rotation. *Icarus* **93**, 288–297.
- Malhotra, R. 1993. The origin of Pluto’s peculiar orbit. *Nature* **365**, 819.
- Malhotra, R. 1995. The origin of Pluto’s orbit: Implications for the Solar System beyond Neptune. *Astron. J.* **110**, 420–429.
- Nesvorný, D., L. Dones, and H. Levison 2002. Orbital dynamics of the irregular satellites. *Astron. J.*, submitted for publication.
- Pollack, J. B., J. A. Burns, and M. E. Tauber 1979. Gas drag in primordial circumplanetary envelopes—A mechanism for satellite capture. *Icarus* **37**, 587–611.
- Pollack, J. B., O. Hubickyj, P. Bodenheimer, J. J. Lissauer, M. Podolak, and Y. Greenzweig 1996. Formation of the giant planets by concurrent accretion of solids and gas. *Icarus* **124**, 62–85.
- Slattery, W. L., W. Benz, and A. G. W. Cameron 1992. Giant impacts on a primitive Uranus. *Icarus* **99**, 167–174.
- Thommes, E. W., M. J. Duncan, and H. F. Levison 1999. The formation of Uranus and Neptune in the Jupiter–Saturn region of the Solar System. *Nature* **402**, 635–638.
- Wetherill, G. W. 1975. Late heavy bombardment of the Moon and terrestrial planets. In *Proc. Lunar Sci. Conf.*, Vol. 6, pp. 866–868. Pergamon, New York.